Backscattering by Nonspherical Hydrometeors as Calculated by the Coupled-Dipole Method: An Application in Radar Meteorology

CLIFTON E. DUNGEY

Directorate of Technology, Headquarters Air Weather Service, Scott Air Force Base, Illinois

CRAIG F. BOHREN

Department of Meteorology, The Pennsylvania State University, University Park, Pennsylvania

(Manuscript received 5 August 1991, in final form 17 December 1992)

ABSTRACT

The severest test of a theory of scattering by particles is how well it calculates scattering in the backward direction. The coupled-dipole method can be used for accurately calculating backscattering at 94 GHz by hexagonal ice crystals. Backscattering by columns is markedly different from that by plates, which indicates that it might be possible to infer size and shape distributions of ice crystals using recently developed millimeter wave radar.

1. Introduction

Cloud and precipitation remote sensing at 94 GHz (3.2 mm) has become possible only recently because of advances in microwave radar technology (Lhermitte 1987). Pulsed Doppler radar enables meteorologists to observe the motion and growth of small hydrometeors; this is not possible with radars that operate at centimeter wavelengths. For certain rainfall events, the backscattered radar signal is used for determining the wind velocity (Lhermitte 1988). The backscattered signal of the raindrops is calculated using Mie theory; however, this theory is not appropriate for calculating backscattering by nonspherical ice crystals. The objective of this paper is to investigate backscattering by hexagonal ice crystals at 94 GHz using the coupled-dipole method. First, we will briefly discuss the limits of applicability of this method to backscattering over the range of crystal sizes of interest.

The coupled-dipole method has gained increased attention over the last few years as a means to calculate scattering by nonspherical particles. General guidelines on the limitations and applicability of this method have been discussed by, for example, Draine (1988) and O'Brien and Goedecke (1988). While astronomers are interested in the forward scattering of radiation by interstellar grains, scientists and engineers in the field of remote sensing are most often limited to the backscattered signal; therefore, the ability of the coupled-dipole method to calculate backscattering needs to be addressed in more detail.

a. Model background

The coupled-dipole method, which is based on a simple physical description of how a particle scatters electromagnetic waves, has remained essentially unchanged since it was published by Purcell and Pennypacker (1973). Its formulation is based on representing an arbitrary particle by an array of N dipolar subunits arranged on a lattice. The dipolar subunits are sufficiently small to give rise to only electric dipole radiation. Total scattering is then calculated by summing the electromagnetic waves scattered by each dipolar subunit excited by the incident wave as well as the waves scattered to it by all other dipolar subunits. A formal mathematical derivation and a short review of the method have been published recently (Lakhtakia 1990).

Partly owing to the enormous computer storage and CPU time required for modeling particles with large size parameters, the coupled-dipole method has not had a great following. But in the past few years, with faster computers and more efficient programming techniques, an increasing number of people have begun using this relatively simple technique. For example, Goedecke and O'Brien (1988), Flatau et al. (1988, 1990), and Evans and Vivekanandan (1990) examined scattering by ice crystals; Singham et al. (1986b) calculated scattering by chiral particles; and Varadan et al. (1989) computed scattering by anisotropic particles.

Corresponding author address: Clifton E. Dungey, Prod. Improv. Div., Attn. XTX, Direct. of Tech., Dept. of AF, Headquarters Air Weather Service, 102 W. Losey Street, Room 105, Scott Air Force Base, IL 62225-5206.

Some recent modifications made to the coupled-dipole method include more efficient means of calculating scattering by randomly oriented particles (Singham et al. 1986a) and improved solution algorithms (Draine 1988; Flatau et al. 1990; Chiapetta 1980; Singham and Bohren 1988) that permit larger values of N. Dungey and Bohren (1991) presented an alternative method of calculating the electric dipole polarizability of the dipolar subunits that improves the accuracy of scattering calculations.

b. *Organization*

In section 2, we briefly review the sensitivity of backscattering calculations using the coupled-dipole method. Only by knowing the strengths and weaknesses of the method can we proceed to interpret our results with any degree of assurance that we remain within the constraints of all physical premises when modeling the scattering of nonspherical particles.

In section 3, we investigate backscattering of 94-GHz radar by ice crystals. First, we examine characteristics of the backscattering by hexagonal columns. Next, we perform a similar analysis with hexagonal plates. Finally, the results are compared, and we identify advantages of using linearly polarized radar.

2. Backscatter sensitivity

Bad data can be made to look good with a suitable choice of statistics. In a similar fashion, scattering models can appear good if only forward-scattering calculations are compared with analytic solutions. Scattering in the backward direction is the most difficult direction to model. We will briefly review ability of the coupled-dipole method for backscattering calculations.

a. *Shape and size dependence of backscattering*

The coupled-dipole method is a good tool to demonstrate why scattering is most sensitive to particle shape and size in the backward direction. Because the scattered light is the sum of all the waves radiated from the dipolar subunits, the intensity of the scattered light depends on the phase relation among all the radiated waves. When the particle is much smaller than the wavelength of radiation, the phase shift across the particle is negligible and the scattering can be estimated using Rayleigh theory. For larger particles, when the phase shift across the particle cannot be ignored, the coupled-dipole method approximates the scattered electric field by accounting for the interaction of a finite number of waves within the particle. Bohren and Singham (1991) have shown the importance of including the interaction matrix in backscattering calculations.

Similarly, the shape of the particle affects backscattering. The simplest explanation is that the shape will affect the arrangement of the constituent dipoles. In the coupled-dipole method, the representation of a particle's shape by finite arrays of dipoles can make computations of backscattering less precise. Draine (1988) presented a formula for estimating the sphericity of an array of dipoles that represents a sphere. Dungey and Bohren (1991) addressed the question of how well an array of dipoles on a simple cubic lattice represents a spherical particle. Although they showed that small variations in sphericity may affect forward scattering at a Frölich frequency, Dungey (1990) showed that a relation between sphericity and accuracy of backscattering calculations by the coupled-dipole method is not evident.

b. *Limitations of the coupled-dipole method*

Agreement with Mie theory is inversely proportional to the modulus of the complex refractive index, which is due to the influence of higher-order multipoles not accounted for in the coupled-dipole method. This loss of accuracy can be overcome somewhat by increasing the number of dipoles in the array while decreasing their size. Dungey (1990) demonstrated this by comparing backscattering calculations from Mie theory with the coupled-dipole method while modeling a sphere represented by arrays of 461, 739, 1064, and 2320 dipoles. The agreement of backscattering calculations improves when increasing the number of dipoles, but at the expense of increased computer time.

Changing the particle size affects the accuracy of scattering calculations when using the coupled-dipole method. Increasing the particle size requires increasing either the radius or number of dipoles in the array that represents the particle. The latter option is permissible, but the accuracy decreases as the radius of the dipoles increases. The general rule of thumb is that the dipoles should satisfy the criterion that $k_0 a|m| < 0.5$, where k_0 is the free space wavenumber, a is the dipole radius, and $|m|$ is the modulus of the refractive index.

A sphere with a refractive index of $1.878 + i4.76 \times 10^{-4}$ (the refractive index of ice at 94 GHz; Lhermitte 1988) was modeled; its size parameter was varied from 1.0 to 3.0. The sphere was represented by arrays designed to keep $k_0 a|m| < 0.5$. The results in Fig. 1 show good agreement with Mie theory until the size parameter reaches 1.6, where the backscattered signal reaches its first minimum value. The deviation appears again near size parameter of 3.0, which corresponds to the second backscattering minimum. These results are the same whether using the matrix inversion (Singham et al. 1986a) or scattering-order technique.

3. Backscattering of 94-GHz radar by ice crystals

The coupled-dipole method is applicable to studying backscattering of 94-GHz radar by ice crystals for several reasons. First, this method can calculate scattering

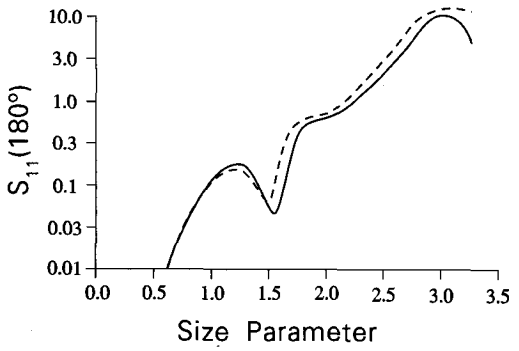

FIG. 1. Comparison of coupled-dipole method with Mie theory for an ice sphere at 94 GHz ($m = 1.878 + i0.0005$). The solid line is calculated results using Mie theory; the dots are from the coupled-dipole method. Term S_{11} represents the total scattered irradiance when the incident light is unpolarized.

by nonspherical ice crystals. Second, the wavelength of this radar is 3.2 mm; hence, the size parameter (or approximately the number of dipoles N needed to represent the particle) is not prohibitively large when modeling particles with linear dimensions of the order of one to five millimeters. Third, when N is on the order of only several hundred, the matrix inversion technique can be used to rotate the particle through many orientations (Singham et al. 1986a). Fourth, the refractive index of ice at this frequency is not too large to prevent use of the scattering-order technique for calculating scattering by larger ice crystals.

The relationship between particle shape and the first backscattering minimum is one of the reasons for studying backscattering at 94 GHz. For falling raindrops, a backscattering minimum occurring at radius 0.83 mm provides an opportunity to remotely identify spherical raindrop size (Lhermitte 1988). This identification is possible because the terminal velocity of raindrops increases with drop radius while backscattering by raindrops is at a local minimum for drop radius 0.83 mm.

Doppler radars measure the line-of-sight (or radial) velocity of their targets (raindrops). When the radar is looking above the horizon (zenith angle less than 90°), the Doppler shift is a result of both the horizontal and vertical motion of the target. The Doppler shift of a falling raindrop increases with drop size because terminal velocity increases with drop size. If we assume some raindrop size distribution, such as the Marshall–Palmer (1948), the relationship between the backscattering for each raindrop size and its corresponding Doppler shift can be determined. The crucial point is that with this raindrop size distribution, the backscattering minima are also present as minima in the Doppler shift spectrum. When we observe the first minimum in the Doppler shift spectrum, we can estimate the portion of the Doppler shift that is caused by falling of the raindrops because the terminal velocity of the raindrops associated with the minimum is known. By mathematically removing that component of motion from the Doppler shift, the clear-air component remains and can provide a better estimate of the clear-air velocity. This information about air motion may help to better understand cloud dynamics, cloud structure, and precipitation processes.

Lhermitte's procedure is based on identifying the backscattering minimum that occurs for spheres. If a backscattering minimum is present for a size distribution of ice crystals, this procedure could increase our understanding of ice clouds. Since ice crystals are nonspherical, Mie theory is not an applicable modeling tool; therefore, an alternative model such as the coupled-dipole method is required. Before calculating backscattering of 94-GHz radar by ice crystals, the accuracy of the coupled-dipole method will be estimated by first comparing scattering results for ice spheres with Mie theory.

a. Ice spheres

The scattering-order technique was used to calculate backscattering by ice spheres, and the results were compared with Mie theory. The refractive index of ice (0°C) at 94 GHz is $1.878 + i4.76 \times 10^{-4}$ (Lhermitte 1988). The number of dipoles in the arrays used to represent the sphere ranged from 461 for the smallest sphere to 2320 for the largest sphere. The number of dipoles was increased to keep the dipole radius small;

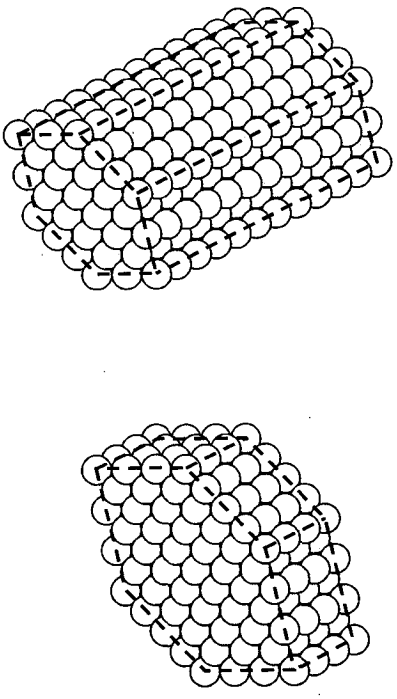

FIG. 2. Arrays of dipoles arranged to represent hexagonal crystals. The top array contains 336 dipoles and represents a 2 × 1 hexagonal column; the bottom array contains 212 dipoles and represents a 2 × 1 hexagonal plate.

this improves the accuracy of the calculations. The results shown in Fig. 2 indicate that calculations by the coupled-dipole method do fairly well at identifying the correct size parameter and magnitude of the backscattering response at the first minimum, and that the agreement with Mie theory decreases for the largest size parameters shown.

b. *Hexagonal columns*

The first ice crystal selected to be modeled is a hexagonal column with aspect ratio 3.5:1, that is, ratio of length to cross section of equivalent area circle. Figure 2 shows examples of hexagonal crystals modeled in the coupled-dipole method. Hexagonal prismatic is the basic shape of ice crystals, although laboratory observations have revealed a few other shapes and a variety of aspect ratios (Pruppacher and Klett 1980, chapter 2). The aspect ratio of 5:1 for the column would have been a better representation based on observations, but computer memory requirements restricted the size.

Calculations were made to determine the shape and size dependence of the first backscatter minimum for ice crystals. Scattering calculations were made with these particles in orientations that simulate natural conditions. Except for very large ice crystals under turbulent conditions (Cho et al. 1981; Pruppacher and Klett 1980) and for very small ice crystals due to Brownian motion (Fraser 1979), ice crystals are expected to fall without tumbling; therefore, the long axis of the particles modeled here remain horizontal. Scattering calculations were made with the long axis at numerous orientations within the x–y plane to simulate particle rotation.

The relationship between polarization of the incident and scattered waves was analyzed using principles associated with the Mueller matrix. The term S_{11} represents the total scattered irradiance when the incident is unpolarized; S_{HH} is the horizontally polarized scattered radiation when the incident radiation is horizontally polarized; S_{VV} is the vertically polarized scattered radiation when the incident radiation is vertically polarized. Horizontal and vertical are defined with respect to the direction of wave propagation and horizon. For this paper, 180° signifies backscatter values.

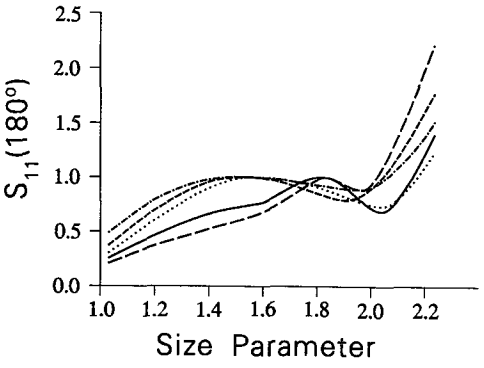

FIG. 3. Backscattering of unpolarized 94-GHz radiation by ice columns of increasing size parameter at various zenith angles. The local maximum value in the curves have been normalized to 1.0. The short-dashed line (- - -) represents a zenith angle of 10°, the dot–dash line (- · - · -) a zenith angle of 30°, the dotted line a zenith angle of 50°, the solid line a zenith angle of 70°, and the long-dashed line (— — —) a zenith angle of 90°.

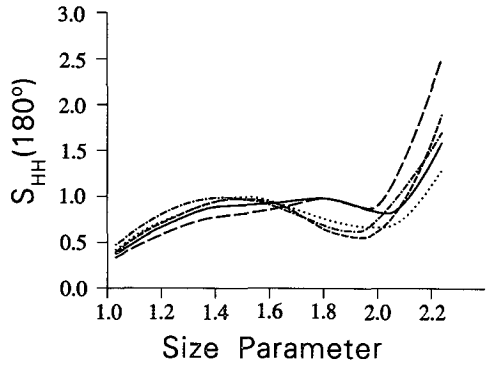

FIG. 4. Backscattering of horizontally polarized 94-GHz radiation by ice columns of increasing size parameter at various zenith angles. The short-dashed line (- - -) represents a zenith angle of 10°, the dot–dash line (- · - · -) a zenith angle of 30°, the dotted line a zenith angle of 50°, the solid line a zenith angle of 70°, and the long-dashed line (— — —) a zenith angle of 90°.

Figures 3–6 show the dependence of backscattering by the hexagonal column (aspect ratio of 3.5:1) on size parameter, which is based on that of an equal-volume sphere. The values for size parameter range from 1.0 to 2.2 and correspond to column lengths of 2.1–4.6 mm. The five lines in the figures represent zenith angles of 10°, 30°, 50°, 70°, and 90°. The local maximum has been normalized to 1.0 for comparing relative changes in the backscattering signal. In all cases the normalization factor is less than two, and the unnormalized value for 10° the largest. Normalized backscatter values of $S_{11}(180°)$ are shown in Fig. 3. For the zenith angles 30° and 90°, the relative difference between the local maximum and minimum is small, and it is largest for 50° and 70°. The shapes of the curves are somewhat different for values of $S_{HH}(180°)$ and $S_{VV}(180°)$ (shown in Figs. 4 and 5). The relative difference between the local maximum and minimum for the $S_{HH}(180°)$ curves are more pronounced for the smallest zenith angles. For $S_{VV}(180°)$ the relative difference between local maximum and minimum is similar for all angles except 90°, but the noticeable feature is the narrowing of the local maximum feature at the two largest zenith angles. A comparison of the backscattering signal at 70° for all three states of polarization is shown in Fig. 6. The most pronounced local minimum is near a size parameter of 2.0 for $S_{VV}(180°)$. The comparison of the backscattering signals in Figs. 3 through 5 agrees with one's intuition that linearly polarized microwave radar (in particular S_{VV}) would

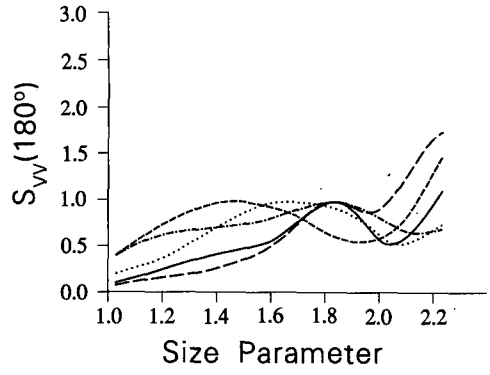

FIG. 5. Backscattering of vertically polarized 94-GHz radiation by ice columns of increasing size parameter at various zenith angles. The short-dashed line (- - -) represents a zenith angle of 10°, the dot–dash line (- · - · -) a zenith angle of 30°, the dotted line a zenith angle of 50°, the solid line a zenith angle of 70°, and the long-dashed line (— — —) a zenith angle of 90°.

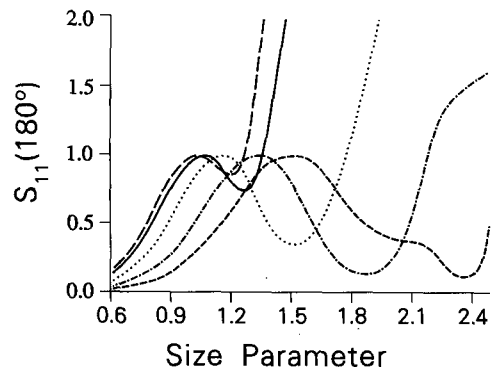

FIG. 7. Backscattering of unpolarized 94-GHz radiation by ice plates of increasing size parameter at various zenith angles. The short-dashed line (- - -) represents a zenith angle of 10°, the dot–dash line (- · - · -) a zenith angle of 30°, the dotted line a zenith angle of 50°, the solid line a zenith angle of 70°, and the long-dashed line (— — —) a zenith angle of 90°.

produce better definition in the backscattering curves. This is also evident in backscattering by ice plates.

Figures 7–10 show the dependence of backscattering by the hexagonal plate (aspect ratio of 1:3.2) on size parameter. The size parameter is again based on an equal-volume sphere. The values for size parameter range from 0.6 to 2.4 and correspond to plates with equivalent-circle diameters of 0.8–3.3 mm. The five lines in the figures represent zenith angles of 10°, 30°, 50°, 70°, and 90°. Normalized values of $S_{11}(180°)$ are shown in Fig. 7. Unlike the results for the hexagonal column, the backscattering minimum for the plate is spread over a larger range of size parameters, and occurs at a lower size parameter for higher zenith angles. The relative difference between the local maximum and local minimum also decreases with increasing zenith angle. For values of $S_{HH}(180°)$ and $S_{VV}(180°)$ (shown in Figs. 8 and 9) the shapes of the curves are again dissimilar for different zenith angles. The main difference between $S_{HH}(180°)$ and $S_{11}(180°)$ is a slight deepening of the backscattering minimum at a zenith angle of 50°. The noticeable differences between $S_{VV}(180°)$ and $S_{11}(180°)$ are the shallower minimum at zenith angle of 50° and the presence of the second backscattering minimum for all zenith angles except 10° and 90° (a shallow minimum occurs at 70°, but it is out of range of the figure). A comparison of the backscattering signal at 50° for all three states of polarization is shown in Fig. 10. In contrast with the results for the hexagonal column, $S_{HH}(180°)$ produces the largest relative difference between the local maximum and minimum.

The backscattering minima for ice crystals have an added feature over their counterparts for spherical raindrops: a dependence on zenith angle. This dependence disappears if the ice crystals tumble as they fall;

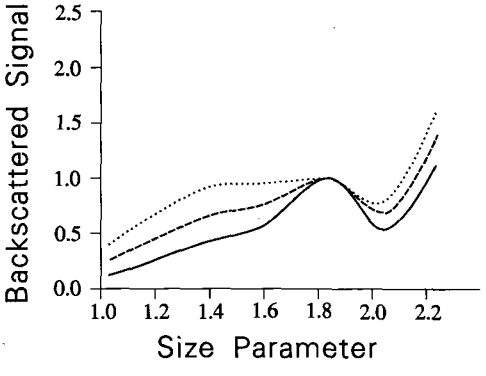

FIG. 6. Backscattering by ice columns of increasing size parameter at zenith angle of 70°. The dashed line represents unpolarized radiation, the dotted line represents horizontally polarized radiation, and the solid line represents vertically polarized radiation.

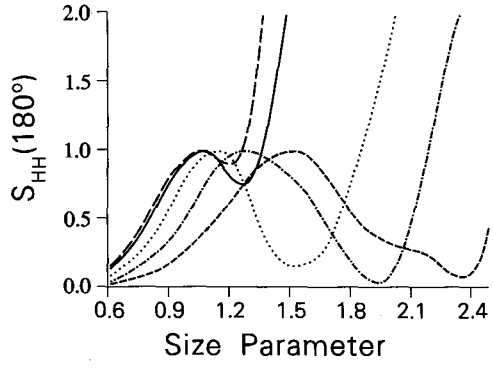

FIG. 8. Backscattering of horizontally polarized 94-GHz radiation by ice plates of increasing size parameter at various zenith angles. The short-dashed line (- - -) represents a zenith angle of 10°, the dot–dash line (- · - · -) a zenith angle of 30°, the dotted line a zenith angle of 50°, the solid line a zenith angle of 70°, and the long-dashed line (— — —) a zenith angle of 90°.

nonetheless, its absence could provide information about turbulence in the vicinity of the crystals. Thus, backscattered signals collected while the radar sweeps through zenith angles may be useful in remotely sensing the atmosphere.

4. Conclusions

Although identification of size and shape distributions of ice crystals using this procedure seems feasible, several contributing technological factors are still uncertain. The technology required to build millimeter-wavelength radar is relatively new. Current research and development of millimeter wave tubes are expected to result in construction of more powerful transmitters (Lhermitte 1990), thereby increasing the sensitivity of the radar. The size range of ice crystals considered in this paper is typical of falling snow. To identify the size distribution of smaller ice crystals, a shorter wavelength is required. A recently developed 1.4-mm (215 GHz) wavelength radar (Mead et al. 1989) has the potential for observing the first minimum in backscattering by smaller ice crystals; however, at this wavelength attenuation by atmospheric water vapor may (depending on the transmission power) limit the system's performance.

Identification of ice-crystal size distribution depends on several other factors. First, the size distribution is assumed to be continuous. A discontinuous size distribution would produce gaps in the Doppler shift spectrum that could be mistaken for a backscattering minimum. Second, selection of a single relationship between fall velocity and size parameter is difficult because of the variety of aspect ratios and crystal shapes. Third, for the theory to be applicable, ice crystals must not be aggregated. Backscattering calculations are made only for plates and columns; scattering by aggregates may obscure the desired backscattering minima. Fourth, the optical depth of the ice cloud must not be too large, otherwise the backscattered signal will be a result of multiple scattering events. The procedure for identifying ice crystals is based on single scattering.

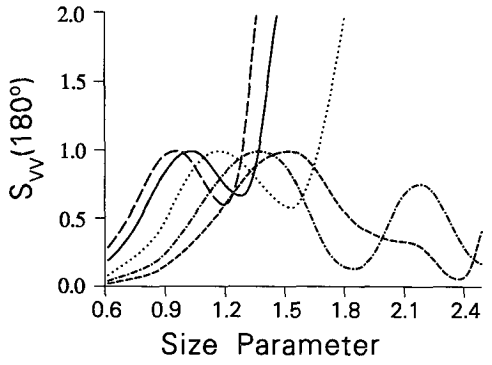

FIG. 9. Backscattering of vertically polarized 94-GHz radiation by ice plates of increasing size parameter at various zenith angles. The short-dashed line (- - -) represents a zenith angle of 10°, the dot-dash line (- · - · -) a zenith angle of 30°, the dotted line a zenith angle of 50°, the solid line a zenith angle of 70°, and the long-dashed line (— — —) a zenith angle of 90°.

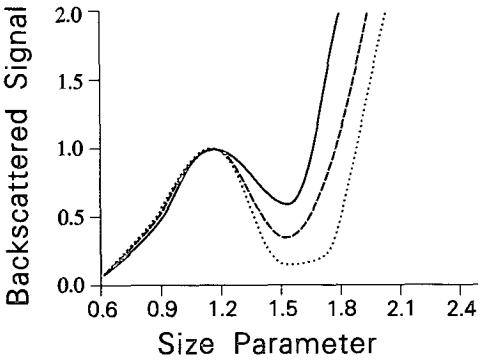

FIG. 10. Backscattering by ice plates of increasing size parameter at zenith angle of 50°. The dashed line represents unpolarized radiation, the dotted line represents horizontally polarized radiation, and the solid line represents vertically polarized radiation.

In this paper, the ability of the coupled-dipole method to calculate backscattering by nonspherical particles was demonstrated. For spheres smaller than the size that produces the first backscattering minimum, small shape variations in the dipolar array do not affect the accuracy of the backscattering calculation. Conversely, when the spheres are larger than the size that produces the first backscattering minimum, backscattering calculations lose accuracy. For particles with a large aspect ratio (at least 5:1) and small size parameter, the backscattering calculation is relatively insensitive to the exact cross-sectional shape of the particle, that is, hexagonal column, cylinder, etc. Finally, backscattering calculations for hexagonal columns and plates have been presented. It is feasible that a size distribution of ice crystals could be estimated using remote sensing techniques. This theory should also be valid for observing cirrus crystals with an instrument operating at a shorter wavelength. In general, the size of the ice crystals will dictate the wavelength that will be best suited for obtaining the first backscattering minimum.

Acknowledgments. We thank Shermila Singham, who provided the original version of the coupled-dipole program that we adapted for use in this project. We also thank Akhlesh Lakhtakia, Tom Ackerman, Sabih Hayek, and Andrew Vogelmann for their time and comments, and Frank Evans for providing similar output from his scattering program. This research was supported in part by National Aeronautics and Space Administration Grant NAS8-36194 and National Science Foundation Grant ATM-8810876.

REFERENCES

Bohren, C. F., and S. B. Singham, 1991: Backscattering by nonspherical particles: A review of methods; suggested new approaches. *J. Geophys. Res.*, **96**(D3), 5269–5277.

Chiapetta, P., 1980: Multiple scattering approach to light scattering by arbitrarily shaped particles. *J. Phys. A*, **13**, 2101–2108.

Cho, H. R., J. V. Iribarne, and W. G. Richards, 1981: On the orientation of ice crystals in a cumulonimbus cloud. *J. Atmos. Sci.*, **38**, 1111–1114.

Draine, B. T., 1988: The discrete-dipole approximation and its application to interstellar graphite grains. *Astrophys. J.*, **333**, 848–872.

Dungey, C. E., 1990: Backscattering by nonspherical particles, using the coupled-dipole method: An application in radar meteorology. Ph.D. thesis, Department of Meteorology, The Pennsylvania State University, University Park, PA, 140 pp.

——, and C. F. Bohren, 1991: Light scattering by nonspherical particles: A refinement to the coupled-dipole method. *J. Opt. Soc. Amer. A*, **8**, 81–87.

Evans, K. F., and J. Vivekanandan, 1990. Multiparameter radar and microwave radiative transfer modeling of non-spherical atmospheric ice particles. *IEEE Geosci. Remote Sens.*, **28**, 423–437.

Flatau, P. T., G. L. Stephens, and B. T. Draine, 1988: Scattering on hexagonal ice crystals: Discrete dipole and anomalous diffraction approximations. *Proc. of the Int. Radiation Symp.*, Lille, France, J. Lenoble and J.-F. Geleyn, Eds., Deepak, 72–75.

——, ——, and ——, 1990: Light scattering by rectangular solids in the discrete dipole approximation: a new algorithm exploiting the block-Toeplitz structure. *J. Opt. Soc. Amer. A*, 7, 593–600.

Fraser, A. B., 1979: What size of ice crystals causes the halos? *J. Opt. Soc. Amer.*, **69**(8), 1112–1118.

Goedecke, G. H., and S. G. O'Brien, 1988: Scattering by irregular inhomogeneous particles via the digitized Green's function algorithm. *Appl. Optics*, **27**, 2431–2438.

Lakhtakia, A., 1990: Macroscopic theory of the coupled dipole approximation method. *Optics Communication*, **79**, 1–5.

Lhermitte, R. M., 1987: A 94-GHz Doppler radar for cloud observations. *J. Atmos. Oceanic Technol.*, **4**, 36–48.

——, 1988: Cloud and precipitation remote sensing at 94 GHz. *IEEE Trans. Geosci. Remote Sens.*, **26**, 207–216.

——, 1990: Attenuation and scattering of millimeter wavelength radiation by clouds and precipitation. *J. Atmos. Oceanic Technol.*, **7**, 464–479.

Marshall, J. S., and W. M. Palmer, 1948: The distribution of raindrops with size. *J. Meteor.*, **5**, 165–168.

Mead, J. B., R. E. McIntosh, D. Vandemark, and C. T. Swift, 1989: Remote sensing of clouds and fog with a 1.4-mm radar. *J. Atmos. Oceanic Technol.*, **6**, 1090–1097.

Mugnai, A., and W. J. Wiscombe, 1980: Scattering of radiation by moderately nonspherical particles. *J. Atmos. Sci.*, **37**, 1291–1307.

Pruppacher, H. R., and J. D. Klett, 1980: *Microphysics of Clouds and Precipitation.* D. Reidel, 713 pp.

Purcell, E. M., and C. R. Pennypacker, 1973: Scattering and absorption of light by nonspherical dielectric grains. *Astrophys. J.*, **186**, 705–714.

Rusk, A. N., D. Williams, and M. R. Querry, 1971: Optical constants of water in the infrared. *J. Opt. Soc. Amer.*, **61**, 895–903.

Singham, M. K., S. B. Singham, and G. C. Salzman, 1986a: The scattering matrix for randomly oriented particles. *J. Chemical Phys.*, **85**(7), 3807–3815.

Singham, S. B., and C. F. Bohren, 1988: Light scattering by an arbitrary particle: The scattering-order formulation of the coupled-dipole method. *J. Opt. Soc. Amer. A*, **5**(11), 1867–1872.

——, C. W. Patterson, and G. C. Salzman, 1986b: Polarizabilities for light scattering from chiral particles. *J. Chemical Phys.*, **85**(2), 763–770.

Takano, Y., and S. Asano, 1983: Fraunhofer diffraction by ice crystals suspended in the atmosphere. *J. Meteor. Soc. Japan*, **61**, 289–300.

Varadan, V. V., A. Lakhtakia, and V. K. Varadan, 1989: Scattering by three-dimensional anisotropic scatterers. *IEEE Trans. Antennas and Propagation*, **37**(6), 800–802.

Yeh, C., R. Woo, A. Ishimaru, and J. Armstrong, 1982: Scattering by single ice needles and plates at 30 GHz. *Radio Sci.*, **17**, 1503–1510.